An Experimental and Theoretical Core-Level Study of Tautomerism in Guanine

Oksana Plekan,[†,‡] Vitaliy Feyer,[†] Robert Richter,[†] Marcello Coreno,[§] Gemma Vall-llosera,[||] Kevin C. Prince,*[,†,⊥] Alexander B. Trofimov,[#,▽] Irina L. Zaytseva,[#] Tatyana E. Moskovskaya,[#] Evgeniy V. Gromov,[#,○] and Jochen Schirmer[○]

Sincrotrone Trieste, in Area Science Park, I-34012 Basovizza (Trieste), Italy, CNR-IMIP, I-00016 Montelibretti (Rome), Italy, Department of Physics, School of Engineering Science, Royal Institute of Technology, 10691 Stockholm, Sweden, Laboratorio Nazionale TASC, INFM-CNR, 34012 Trieste, Italy, Laboratory of Quantum Chemistry, Irkutsk State University, 664003 Irkutsk, Russia, Favorsky Institute of Chemistry, SB RAS, 664033 Irkutsk, Russia, and Theoretische Chemie, Physikalisch-Chemisches Institut, Universität Heidelberg, Im Neuenheimer Feld 229, D-69120 Heidelberg, Germany

Received: April 7, 2009; Revised Manuscript Received: June 30, 2009

The core level photoemission and near edge X-ray photoabsorption spectra of guanine in the gas phase have been measured and the results interpreted with the aid of high level ab initio calculations. Tautomers are clearly identified spectroscopically, and their relative free energies and Boltzmann populations at the temperature of the experiment (600 K) have been calculated and compared with the experimental results and with previous calculations. We obtain good agreement between experiment and the Boltzmann weighted theoretical photoemission spectra, which allows a quantitative determination of the ratio of oxo to hydroxy tautomer populations. For the photoabsorption spectra, good agreement is found for the C 1s and O 1s spectra but only fair agreement for the N 1s edge.

I. Introduction

Tautomerism is a form of isomerism which occurs in some nucleic acid bases and may have some relevance to genetic mutations, when rare tautomers are incorporated into genetic material. Of the five nucleic acid bases present in DNA and RNA, guanine and cytosine have significant populations of two or more tautomers in the gas phase, whereas uracil, adenine, and thymine exist only as single isomers.[1−7] The most important types of tautomerism in this class of compounds are amino−oxo, amino−hydroxy, and amino−imino forms. Further conformers (rotamers) exist, based on rotation of hydroxyl and imine groups to give cis and trans isomers. There have been several experimental studies of free or matrix isolated guanine and cytosine aiming at identifying the species present, and employing laser, microwave, infrared, and vibrational spectroscopy. In addition a number of theoretical studies have sought to determine the structures and relative free energies of their guanine and cytosine isomers.[8−13] Several notations have been used for the tautomers of guanine, and we adopt the labeling of Marian,[9] Figure 1.

Piuzzi et al.[3] and Mons et al.[6] used laser spectroscopy and observed tautomers **1**, **2**, **5**, and either **3** or **4** but could not reconcile the abundances with calculated values. Indeed differences in the spectral intensities suggested that the populations of the tautomers depended on the method of evaporation, and this dependence has recently been confirmed in a photoionization study.[14] Nir et al.[4] also used laser desorption and laser spectroscopy and observed tautomers **1**, **2**, and **3**. Choi and Miller[1] observed four tautomers in helium nanodroplets using infrared laser spectroscopy, assigned to **1**, **2**, **3**, and **4**. More recently, several authors[9,11−13] reinterpreted the spectra of refs 3, 4, and 6. Marian[9] reassigned some bands observed by Choi and Miller[1] to tautomers **7** and **8**, although the population of these tautomers was calculated to be very low. These two

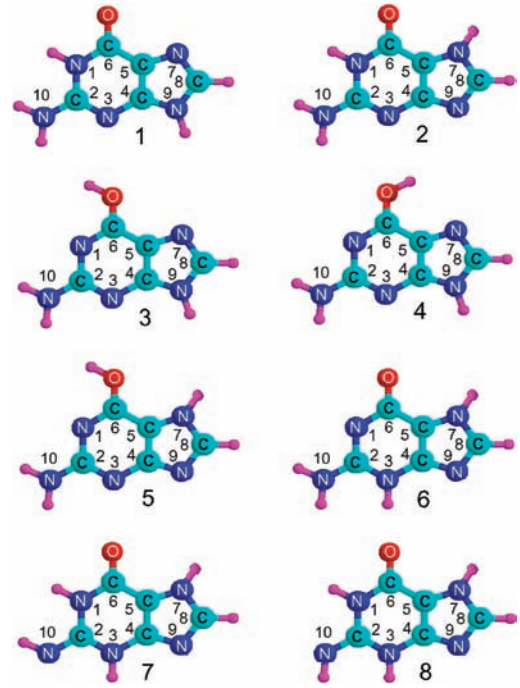

Figure 1. Tautomers of guanine.

* Corresponding author: e-mail, Prince@Elettra.Trieste.It; fax number, +39 040 375 8565.
† Sincrotrone Trieste.
‡ Permanent address: Institute of Electron Physics, 88017 Uzhgorod, Ukraine.
§ CNR-IMIP.
|| Department of Physics, School of Engineering Science, Royal Institute of Technology.
⊥ Laboratorio Nazionale TASC, INFM-CNR.
Laboratory of Quantum Chemistry, Irkutsk State University.
▽ Favorsky Institute of Chemistry, SB RAS.
○ Theoretische Chemie, Physikalisch-Chemisches Institut, Universität Heidelberg.

10.1021/jp903209t CCC: $40.75
Published on Web 07/27/2009

tautomers are imino−hydroxy rotamers of guanine, which were not considered by the three experimental studies.[11−13] The calculated Boltzmann population ratios were different from those of Choi and Miller. Clearly a further independent experimental and theoretical determination of the Boltzmann population ratios is desirable.

Calculations of the relative thermodynamic stability of guanine tautomers have been reported by several authors.[1,8,9,11−13] Choi and Miller[1] employed the second-order Møller−Plesset perturbation theory (MP2) and basis sets 6-311++G(d,p) and aug-cc-pVDZ to evaluate relative free energies for a wide range of temperatures. Hanus et al.[8] used resolution of identity (RI) MP2[15] and a double-polarized triple-ζ (TZVPP) basis set to obtain the optimized ground-state molecular geometries of guanine tautomers. The relative electronic energies were then finalized by adding corrections for higher electron correlation terms estimated using a smaller aug-cc-pVDZ basis set[16] in which the energy differences between the MP2 and more extensive coupled cluster singles and doubles method with noniterative treatment of triple excitations [CCSD(T)] could be evaluated. The thermal corrections were calculated at the MP2/6-31G** level to obtain the relative Gibbs energies for $T =$ 298 K.

As noted above, the eight most stable tautomers of guanine were investigated theoretically by Marian,[9] using the DFT approach. The B3LYP/TZVP[17,18] scheme was employed for geometry optimization, and then the combined DFT/multireference configuration interaction (DFT/MRCI) method[19] was used for refinement of the tautomer energies. Boltzmann population ratios for $T = 900$ K were evaluated for interpretation of IR−UV spectroscopic data.

Core level spectroscopy, the experimental technique used here, has been applied to study tautomers of some volatile smaller molecules,[20,21] but until now it has not been applied successfully to guanine because it is thermally sensitive, and indeed there have been several reports of the difficulty of evaporating guanine (ref 32 in ref 22 and refs 23 and 24). Indeed Nir et al.[25] reported that "guanine in particular cannot be vaporized intact by simple thermal heating...". For this reason, most reported work used jet-cooled samples (where the sample temperature is not well-defined) or matrix isolation and few used thermal evaporation. However, as we show here, guanine can indeed be evaporated without decomposition,[1,26] at a well-defined sample temperature where the populations are in thermal equilibrium.

Our core level photoemission and photoabsorption spectra are accompanied by ab initio calculations. Photoemission has the advantage that to a good approximation the core level signal is directly proportional to the population of the state and the small deviations expected (of the order 10%) can be corrected by theoretical calculations, which also provide an assignment of the spectral features. We have recently reported core level spectra and detailed calculations for adenine and thymine[5] and cytosine and uracil,[27] and the present work continues our research on the five nucleic acid bases.

II. Experimental and Theoretical Methods

Experimental Section. The experimental and theoretical methods have been described in detail elsewhere[5] and here we summarize them briefly. The samples were obtained from Sigma-Aldrich with minimum purity of 99% and used without any further purification. They were evaporated from the same furnace as previously and were checked before the experiment using photoionization mass spectrometry, to ensure that there were no effects due to thermal decomposition. The evaporation temperature was 600 K, with some tests at 575 K, which gave identical spectra with poorer statistics. The spectra were taken at the gas phase photoemission beamline, Elettra, Trieste,[28] using the same apparatus as previously. To check the quality of the samples, valence spectra were taken at 99 eV photon energy. The peak energies were consistent with those of Dougherty[26] measured at 21.2 eV, with different relative peak intensities due to different cross sections. The C 1s, N 1s, and O 1s core photoemission spectra were taken at 382, 495, and 628 eV photon energy, respectively, and the binding energy was calibrated to the 1s energies of N_2 and CO_2.[29,30] The spectra were measured with a total resolution (photons+analyzer) of 0.20, 0.32, 0.46, and 0.53 eV at $h\nu = 99$, 382, 495, and 628 eV, respectively. For the photoabsorption spectra, the resolution was 70, 60, and 100 meV at the C, N, and O edges, respectively, and the energy scales of the spectra were calibrated as in ref 31.

Theoretical Approach. Essentially the same theoretical approach as in our previous study of thymine and adenine[5] was employed, and we summarize it briefly. The energies (Ω_t) and the pole strengths (P) of the vertical ionization transitions were computed using the fourth-order algebraic-diagrammatic construction (ADC(4)) approximation scheme for the one-particle Green's function[32−34] adapted for the case of K-shell ionization by means of an additional core−valence separation (CVS) approximation.[35,36] The pole strengths P represent the outcome of the Green's function theory applied to molecular electronic structure and do not contain any photon energy dependent cross-section effects.[32−35] The 6-31G basis sets[37,38] were used in the calculations. The ionization spectra were calculated using the ADC(4)/CVS one-particle Green's function code[39] interfaced to the GAMESS (UK)[40] and GAMESS (US)[41] program packages.

The energies (Ω_t) and the optical oscillator strengths (f) of the vertical K-shell excitations were evaluated using the second-order algebraic-diagrammatic construction (ADC(2)) approximation scheme for the polarization propagator[42,43] also including the CVS approximation.[44] The 6-31+G basis sets[37,38] including diffuse basis functions were used in these calculations. The calculations were performed using the ADC polarization propagator code[45] interfaced to the GAMESS (US) program.[40]

The ground-state molecular structures of guanine in Figure 1 were obtained by means of a geometry optimization procedure in which density functional theory was employed (DFT) with the B3LYP potential[46] and 6-311G** basis sets.[47] All tautomers were treated as planar molecules; i.e., the out-of-plane bending of the NH_2 group was neglected in species **1**−**6**. The planar approximation permits the use of molecular symmetry of the C_s point group, which is crucial to make the computationally expensive ADC(4) calculations feasible. The interpretation of ADC(2) polarization propagator results is also greatly simplified when guanine can be considered as a planar molecule. This approximation is considered an insignificant perturbation to the final K-shell ionization and excitation spectra. The B3LYP/6-311G** calculations were carried out using the GAUSSIAN program.[48]

The theoretical spectra of guanine were constructed as Boltzmann Population Ratio weighted sums of the spectra obtained for each tautomer. The Boltzmann factors defining population ratios of tautomers at the experimental temperatures were determined from a separate thermochemical study. For this study, the molecular structures of the eight guanine tautomers (Figure 1) were optimized at the MP2 level using the cc-pVTZ basis set[23] (see also Supporting Information). The

TABLE 1: Relative Electronic Energies (kJ/mol) of Guanine Tautomers Computed Using MP2, CCSD, and CCSD(T) Methods with cc-pVTZ and 6-311+G Basis Sets, and Extrapolated Values (MP2+Δ_{Corr} and CCSD+Δ_{Corr})**

	basis set cc-pVTZ				basis set 6-311+G**		
tautomer	MP2	CCSD	MP2+Δ_{Corr}[a]	CCSD+Δ_{Corr}[b]	MP2	CCSD	CCSD(T)
1	1.72	0.71	1.92	1.87	0.96	0.0	1.16
2	0.0	0.0	0.0	0.0	0.0	0.0	0.0
3	1.99	1.78	1.58	1.71	1.27	0.92	0.85
4	3.10	3.71	3.20	3.36	3.84	4.28	3.94
5	15.02	16.19	14.46	14.69	14.39	15.34	13.84
6	26.85	26.67	27.45	27.41	27.23	27.09	27.83
7	30.42	24.84	27.52	27.58	34.97	29.33	32.07
8	30.31	25.08	27.93	28.05	34.70	29.35	32.32

[a] Extrapolated MP2/cc-pVTZ results. The estimates of higher electron correlation effects $\Delta_{Corr} = E(\text{CCSD(T)}) - E(\text{MP2})$ are obtained from the present 6-311+G** basis set calculations. [b] Extrapolated CCSD/cc-pVTZ results. The estimates of higher electron correlation effects $\Delta_{Corr} = E(\text{CCSD(T)}) - E(\text{CCSD})$ are obtained from the present 6-311+G** basis set calculations.

TABLE 2: Theoretical Relative Gibbs Free Energies (kJ/mol) and Boltzmann Population Ratios of Guanine Tautomers at 298 and 600 K

	298 K				600 K		
tautomer	this work[a]	Hanus et al.[b]	Choi and Miller[c]	Marian[d]	this work[a]	Choi and Miller[c]	Marian[d]
				Gibbs Free Energy			
1	1.78	1.84	2.1	5.62	1.81	1.7	5.65
2	0.0	0.0	0.0	0.0	0.0	0.0	0.0
3	1.94	2.34	4.0	4.50	2.53	4.2	5.09
4	3.61	3.64	5.1	4.17	4.00	5.2	4.56
5	13.76	13.75		11.99	13.75		11.98
6	26.25	24.75		31.01	25.19		29.94
7	26.62			26.48	25.86		25.71
8	26.84			29.02	25.88		28.05
				Boltzmann Population Ratios			
1	0.224	0.227	0.24	0.071	0.246	0.28	0.147
2	0.458	0.476	0.57	0.685	0.354	0.40	0.457
3	0.210	0.185	0.12	0.112	0.213	0.17	0.165
4	0.107	0.110	0.07	0.127	0.158	0.14	0.183
5	0.002	0.002		0.005	0.023		0.041
6	0.0	0.0		0.0	0.002		0.001
7	0.0			0.0	0.002		0.003
8	0.0			0.0	0.002		0.002

[a] Values were obtained by combining the MP2+Δ_{Corr} electronic energies (Table 1) with the thermal corrections calculated at the B3LYP/6-311G** level of theory. [b] Reference 8: RI-MP2/TZVPP//RI-MP2/TZVPP relative energies corrected for higher electron correlation terms [CCSD(T)-MP2/aug-cc-pVDZ] with thermal corrections evaluated at the MP2/6-31G** level of theory. [c] Reference 1 (as determined from plots in Figure 2): MP2 treatment using 6-311++G(d,p) and cc-pVDZ basis sets. [d] Reference 9: B3LYP/TZVP level of theory accounting for electron correlation effects within the DFT/MRCI framework. Thermal corrections for $T = 298$ and 600 K were obtained in the present work by repeating appropriate B3LYP/TZVP calculations for these temperatures.

relative energies were then established using the results of the CCSD(T) scheme which accounts for higher electron correlation effects. The more compact triple-ζ 6-311+G** basis set[37,38] was employed in the CCSD(T) calculations. The results of MP2/cc-pVTZ computations for geometries were confirmed by the additional CCSD/cc-pVTZ computations.

The present theoretical intensities of the vertical transitions, accounting for Boltzmann population ratios (BPR) (i.e., $I_t = P \times \text{BPR}$ and $I = f \times \text{BPR}$ in the case of ionization or excitations, respectively), were normalized to unity for the excitation spectra. For the photoionization spectra, the data were normalized to the respective number of atoms in the molecule (1 for oxygen, 5 for nitrogen and carbon). For easier comparison with experimental intensities, I_e, the intensity I_t of each spectrum was calculated by summing the contributions. The spectral envelopes were generated by convoluting the discrete transition lines with Gaussian and Lorentzian lines for ionization and excitation, respectively. A single width was used in each spectrum for all states and all tautomers, although in the experimental spectrum the widths vary. The widths were chosen to match the theoretical spectrum to the experiment and are due to the convolution of experimental resolution, unresolved vibrational structure, and natural lifetime widths. The most decisive comparison is therefore between theoretical and experimental areas; for the theoretical spectra, the peak heights are proportional to the area.

III. Results and Discussion

III.1. Thermochemistry of Guanine. We calculated Gibbs energies and Boltzmann population ratios to compare with the thermodynamic parameters of Choi and Miller,[1] Hanus et al.,[8] and Marian[9] and to compare theory with experiment at the temperature mainly used in the present study, 600 K. The results are summarized in Tables 1 and 2. All molecular geometries were optimized at the MP2/cc-pVTZ level. Table 1 indicates that the relative stabilities of the six lowest energy tautomers change by up to 0.8 kJ/mol as the theoretical treatment is improved from the MP2 to the CCSD(T) level. Even more pronounced effects of electron correlation can be seen for energies of higher-lying tautomers **7** and **8**.

The basis set also seems to play an important role in the description of the guanine tautomers. The present MP2 and CCSD results obtained with the cc-pVTZ and 6-311+G** basis

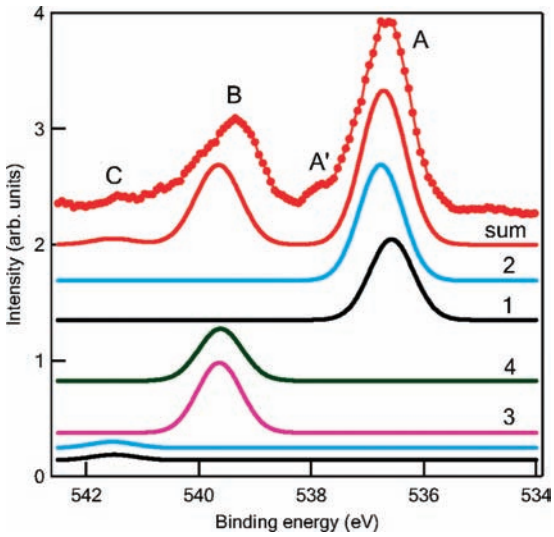

Figure 2. Experimental O 1s photoemission spectrum of guanine (points and lines) and theoretical spectra (lines) of the four most highly populated tautomers and their sum: bottom two curves, spectra of satellites (see text); shift of theoretical spectrum, −1.0 eV; Gaussian broadening, 1.0 eV.

sets differ from each other quite appreciably, and this is especially evident in the case of tautomers **7** and **8**. This indicates that the results for relative stabilities of guanine tautomers are still not sufficiently converged at the present triple-ζ level of theory. In such a situation the larger cc-pVTZ set might be somewhat more reliable.

On this assumption, we use the present MP2/cc-pVTZ energies as a starting point for our thermochemical analysis. To these values we add corrections due to higher electron correlation effects (estimated as differences of the MP2 and CCSD(T) energies for the 6-311+G** basis set) and further terms contributing to Gibbs free energies (evaluated at the B3LYP/6-311G** level of theory): zero-point vibrational energies (ZPVE), temperature-dependent enthalpies and entropies. Using the CCSD/cc-pVTZ calculations, we were able to obtain also the more accurate CCSD+Δ_{Corr} result (accounting for the energy change from CCSD to CCSD(T) treatments for the 6-311G** basis set). As seen from Table 1, the CCSD+Δ_{Corr} and MP2+Δ_{Corr} energies are in good agreement with each other.

The present relative Gibbs free energies computed for T = 298 K are in good agreement with the earlier predictions of Hanus et al.,[8] and with previous data of Choi and Miller,[1] particularly for tautomers **1** and **2**. Furthermore, the ordering of the tautomers obtained here is the same as in the latter calculations, although tautomers **3** and **4** are predicted in ref 1 at somewhat higher energy (Table 2). Although the present and previous results[1,8] are quite consistent, very different relative energies were obtained in the most recent theoretical study of Marian.[9] Here, the ordering of tautomers is **2**, **4**, **3**, **1**, **5**, **7**, **8**, **6**, which is at variance with most other studies of guanine tautomers. Similar observations apply for T = 600 K where again our results are quite consistent with the data of Choi and Miller[1] but differ qualitatively from those of Marian.[9]

The data of Table 2 show that in the gas phase at room temperature, the energetically lowest form **2** of guanine is less than 2 kJ/mol more stable than the nearly degenerate forms **1** and **3**, which lie below tautomer **4**. There are altogether four tautomers whose energies are within 4 kJ/mol of each other, and furthermore, tautomers **5**−**8** lie distinctly higher in energy and are not significantly populated at room and experimental temperatures, Table 2.

TABLE 3: Calculated ($I \geq 0.01$) and Experimental O 1s Ionization Energies and Intensities of Guanine

Theory						Experiment		
Tautomer	Transition	Ionization energy[a] Ω_t	Pole strength P	I^b	I_t^b	Feature	Area, I_e	Ω_e
1	$(O\ 1s)^{-1}$	536.57	0.493	0.224	0.55	A	0.58±0.03	536.7
2	$(O\ 1s)^{-1}$	536.76	0.495	0.323				
	?					A'	0.04±0.02	537.9
4	$(O\ 1s)^{-1}$	539.61	0.578	0.169		B	0.35±0.03	539.4
3	$(O\ 1s)^{-1}$	539.63	0.577	0.227	0.42			
5	$(O\ 1s)^{-1}$	540.01	0.578	0.024				
1	$(O\ 1s)^{-1}(\pi_7)^{-1}(\pi_8^*)^1$	541.50	0.032	0.015	0.03	C	0.04±0.02	541.4
2	$(O\ 1s)^{-1}(\pi_7)^{-1}(\pi_8^*)^1$	541.53	0.026	0.017				

[a] The values of Ω_t have been shifted by −1.00 eV to align the energy axes. [b] I_t and I_e have been normalized to sum to unity.

As expected, at 600 K the present theoretical ratio of tautomers **1**, **2**, **3**, and **4** is more uniform than at 298 K, and is 0.246:0.354:0.213:0.158. The presently predicted ratio is in fair agreement with that following from relative energies of Choi and Miller[1] but, as expected, differs qualitatively from that derived from the data of Marian.[9]

III.2. O, N, and C 1s Ionization Spectra of Guanine. Figure 2 and Table 3 compare the theoretical and experimental results for the O 1s ionization of guanine. The theoretical spectrum has been shifted by −1.0 eV to align the peaks and is in good qualitative agreement with the experimental envelope. The two experimental maxima A and B are well reproduced by the present theoretical modeling, and the feature C due to satellite states is also well reproduced. The feature A′, with an intensity of a few percent, is of unknown origin. The calculated intensity ratio A:B:C = 0.55:0.42:0.03 is in quite good agreement with the ratio of experimental peak areas, 0.58:0.35:0.04. (The last ratio does not sum to unity because of the weak, unassigned feature A′.) Our results indicate clearly that the low energy peak A is formed by the O $1s^{-1}$ ionization signals of oxo-type tautomers **1** and **2**, whereas the higher energy peak B consists of signals from hydoxy-type tautomers **3**, **4**, and to some extent **5**. The remaining oxo-type tautomers, **6**, **7**, and **8**, according to our calculations also contribute to band A, though with negligible intensities due to their very low abundance (see Supporting Information). The energies are consistent with those of oxo and hydroxy groups in other organic molecules.[49]

Our calculations predict various two-hole, one-particle (2h−1p) photoelectron satellites, most of which have very small spectral intensities. There are however two transitions associated with species **1** and **2**, respectively, which we have assigned in Table 3 to the weak maximum C at 540.7 eV. These 2h−1p satellites can be viewed as ionization of the O 1s orbitals plus $\pi-\pi^*$ excitations from the highest occupied to the lowest unoccupied molecular orbitals (MO). The experimental O 1s binding energy of tautomer **1** is in very good agreement with the calculation of Takahata et al.[50] However these authors calculated only this tautomer.

In guanine there are five inequivalent nitrogen atoms, so that the four principle tautomers give rise to a total of 20 ionization lines which are listed in Table 4. These transitions can be subdivided into two groups, imino and amino. The 10 imino-type nitrogen atoms (N_3, N_7 in tautomer **1**, N_3, N_9 in tautomer **2**, N_1, N_3, N_7 in tautomers **3** and **4**) have lower binding energies than the six amino-type atoms (N_1, N_9 in tautomer **1**, N_1, N_7 in tautomer **2**, N_9 in tautomers **3** and **4**). While all the nitrogen atoms (except for the isolated N_{10} amino nitrogen) are incor-

TABLE 4: Calculated ($I \geq 0.04$) and Experimental N 1s Ionization Energies and Intensities of Guanine

Theory						Experiment		
Tautomer	Transition	Ω_t[a]	P	I[b]	I_t[d]	Maximum	I_e	Ω_e
2	$(N_3\ 1s)^{-1}$	404.13	0.551	0.354				
4	$(N_1\ 1s)^{-1}$	404.34	0.548	0.158				
4	$(N_3\ 1s)^{-1}$	404.35	0.542	0.156				
3	$(N_3\ 1s)^{-1}$	404.37	0.543	0.210				
2	$(N_9\ 1s)^{-1}$	404.42	0.546	0.351	2.15	A	2.0	404.5
3	$(N_1\ 1s)^{-1}$	404.49	0.550	0.213				
1	$(N_3\ 1s)^{-1}$	404.51	0.555	0.248				
1	$(N_7\ 1s)^{-1}$	404.63	0.553	0.248				
3	$(N_7\ 1s)^{-1}$	404.74	0.547	0.212				
4	$(N_7\ 1s)^{-1}$	405.04	0.547	0.158				
4	$(N_{10}\ 1s)^{-1}$	405.34	0.589	0.170	0.56	B	–	405.1
3	$(N_{10}\ 1s)^{-1}$	405.46	0.589	0.228				
2	$(N_{10}\ 1s)^{-1}$	406.14	0.596	0.383				
1	$(N_1\ 1s)^{-1}$	406.21	0.582	0.260				
2	$(N_1\ 1s)^{-1}$	406.33	0.583	0.375				
3	$(N_9\ 1s)^{-1}$	406.37	0.576	0.223	2.29	C	3.0	406.3
1	$(N_{10}\ 1s)^{-1}$	406.38	0.590	0.264				
1	$(N_9\ 1s)^{-1}$	406.40	0.578	0.259				
4	$(N_9\ 1s)^{-1}$	406.58	0.575	0.166				
2	$(N_7\ 1s)^{-1}$	406.66	0.566	0.364				

[a] The values of Ω_t have been shifted by −1.41 eV to align the energy scales. [b] The theoretical (I_t) and experimental (I_e) intensities have been normalized to sum to 5.

porated into conjugated electronic systems, there is a difference between the amino and imino species, the former contributing two (lone pair) electrons each to the π-system, whereas in the case of the imino nitrogens (with σ-type in-plane lone pair orbitals) only one electron each is committed to the π-system. The partial delocalization of the π-electrons results in a net charge loss of the amino-type nitrogens as compared to the imino-type atoms, which in turn is reflected in the distinctly larger binding energies of the amino-type N 1s electrons.[5] Accordingly, the N 1s ionization spectrum exhibits two distinct maxima A and C, Figure 3, of approximately equal intensity separated by an energy interval of about 2 eV.

The theoretical spectrum is in good agreement with the experimental data, and the weak shoulder B is also reproduced. This originates essentially from 1s ionization of the NH_2 group, N_{10}, of tautomers **3** and **4**. The N_{10} atoms are outside the heterocyclic system and might be expected to have a relatively constant binding energy in all tautomers. This is however not confirmed by our calculation, and instead the N_{10} 1s binding energy in tautomers **3** and **4** is distinctly lower than those in tautomers **1** and **2**. This underlines some differences in the electronic structure of the NH_2 group in these tautomers. For example, in tautomers **3** and **4**, intramolecular hydrogen bonding of the hydrogen atoms of the NH_2 group with the lone pair of the N_1 atom cannot be excluded. Here we note that the varying N_{10} binding energy as well as any residual discrepancy between the calculated and experimental N 1s spectrum might be an artifact of the present calculations related to the assumption of planar guanine structure (and more specifically of the NH_2 group). The planar structure may favor conjugation of the NH_2 lone pair with the π-density of the ring fragment (i.e., may lead

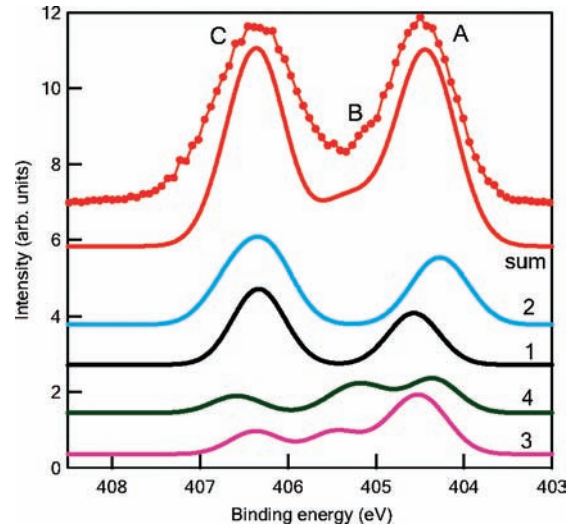

Figure 3. Experimental N 1s photoemission spectrum of guanine (points and lines) and theoretical spectra (lines) of the four most highly populated tautomers and their sum: shift of theoretical spectrum, −1.41 eV; Gaussian broadening, 0.66 eV.

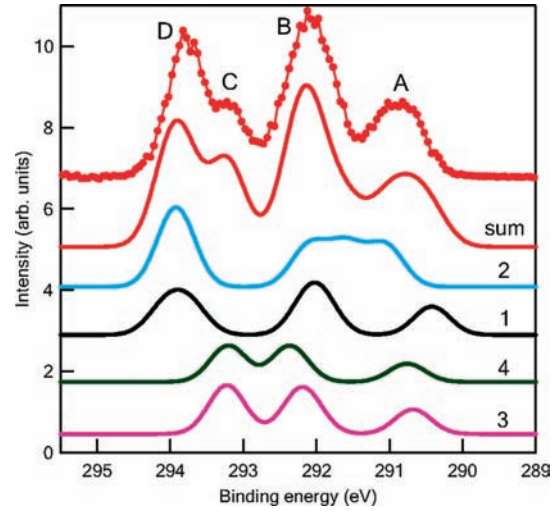

Figure 4. Experimental C 1s photoemission spectrum of guanine (top curve, points and lines) and theoretical spectra (lines) of the four most highly populated tautomers and their sum: shift of theoretical spectrum, −1.55 eV; Gaussian broadening, 0.6 eV.

to an overestimation of the electronic interaction of the NH_2 and ring fragments).

Since the feature B is not well-resolved experimentally, it is difficult to compare integral intensities. Fitting the spectrum to obtain a ratio of peak C to A + B, we obtain a value of 2.0:3.0, compared with the calculated value of 2.7:2.3, which is only in fair agreement.

Takahata et al.[50] calculated the N 1s binding energies of tautomer **1** and predicted two peaks of average energy 404.6 and 406.5 eV, in quite good agreement with the experimental results. However they did not predict peak B, as it does not arise from this tautomer.

The C 1s ionization spectrum of guanine (Figure 4, Table 5) exhibits four clear maxima. In guanine there are no tautomers due to migration of hydrogen atoms attached to carbon, and so corresponding C atoms of different tautomers will not have very different chemical shifts due directly to hydrogen migration. However between the oxo and hydroxy tautomers the C_6 to O bond changes from double to single, and the C_6N_1 bond from single to double (lactam−lactim tautomerism). Thus we expect

TABLE 5: Calculated ($I \geq 0.04$) and Experimental C 1s Ionization Energies and Intensities of Guanine

Theory						Experiment		
Tautomer	Transition	Ω_t[a]	P	I	I_t[b]	Maximum	I_e[c]	Ω_e
1	$(C_5\ 1s)^{-1}$	290.42	0.590	0.265	1.04	A	0.99	290.9
3	$(C_5\ 1s)^{-1}$	290.68	0.588	0.229	(1.07)			
4	$(C_5\ 1s)^{-1}$	290.76	0.588	0.170				
2	$(C_5\ 1s)^{-1}$	291.05	0.582	0.376				
2	$(C_4\ 1s)^{-1}$	291.59	0.590	0.381	1.99	B	2.1	292.1
1	$(C_8\ 1s)^{-1}$	291.93	0.538	0.242	(1.98)			
2	$(C_8\ 1s)^{-1}$	292.10	0.548	0.354				
1	$(C_4\ 1s)^{-1}$	292.12	0.584	0.262				
3	$(C_8\ 1s)^{-1}$	292.12	0.532	0.207				
3	$(C_4\ 1s)^{-1}$	292.26	0.582	0.226				
4	$(C_8\ 1s)^{-1}$	292.35	0.523	0.151				
4	$(C_4\ 1s)^{-1}$	292.38	0.585	0.169				
4	$(C_2\ 1s)^{-1}$	293.20	0.570	0.165	0.76	C	0.51	293.15
3	$(C_2\ 1s)^{-1}$	293.20	0.547	0.213	(0.61)			
4	$(C_6\ 1s)^{-1}$	293.21	0.555	0.161				
3	$(C_6\ 1s)^{-1}$	293.25	0.566	0.220				
1	$(C_6\ 1s)^{-1}$	293.73	0.559	0.251	1.21	D	1.41	293.8
2	$(C_2\ 1s)^{-1}$	293.87	0.560	0.361	(1.34)			
2	$(C_6\ 1s)^{-1}$	293.97	0.547	0.353				
1	$(C_2\ 1s)^{-1}$	294.06	0.543	0.244				

[a] The values of Ω_t have been shifted by -1.55 eV to align the energy scales. [b] The sum has been normalized to 5. Numbers in brackets recalculated, as described in text. [c] The sum has been normalized to 5.

that only the C_6 1s line may show a substantial difference between tautomers. As for N 1s, the five nonequivalent C atoms give rise to a total of 20 ionization lines but again, due to accidental (near) degeneracies, only a restricted number of four peaks are observed.

The C 1s theoretical spectrum is in good qualitative agreement with the experimental data. All main features of the experimental spectral profile are satisfactorily reproduced by our calculations. The energy scale of the theoretical spectrum appears expanded with respect to the experimental spectrum, but the intensities are reproduced well. The lowest XPS band A is due to the aromatic C_5 atoms in tautomers **1**−**4** (Table 5), and experimentally only a single band is observed although the calculations predict a range of energies. The energy for tautomer **1** is 290.39 eV and is the lowest binding energy since it is incorporated in the largest conjugated fragment. Tautomers **3** and **4** have a C_5 1s energy of about 290.79 eV, and tautomer **2**, about 291.06 eV.

The spectral maximum B at 292.10 eV originates from ionization of C_4 and C_8 atoms. As seen from Figure 4 all four principle tautomers contribute to this band and their contributions cannot be resolved. Bands C and D with maxima at 293.24 and 293.80 eV, respectively, result from the ionization of C_6 and C_2 atoms. As seen from Figure 4, band C originates from the spectra of tautomers **3** and **4**, while band D combines contributions of tautomers **1** and **2**. The bands C and D can be viewed as a clear signature of tautomers **3** + **4** and **1** + **2** in the C 1s spectrum.

The experimental intensities in Table 5 were calculated by fitting Gaussian peaks to the spectrum, while the calculated intensities I_t which are not in brackets have been calculated by adding the theoretical intensities I. The agreement for the ratios of peaks A and B is excellent, but there are some discrepancies for peaks C and D. We believe this is due to the overlap of the tails of the peaks and the complexity of the spectrum. To test this hypothesis, we took the theoretical spectra constructed from 20 individual contributions and fitted it with only 4 Gaussian peaks, and obtained the intensities I_t in brackets. While the agreement with theory for peaks A and B deteriorates very slightly, for peaks C and D the agreement is much better, thus confirming the accuracy of our intensity calculations.

Takahata et al.[50] predicted C 1s binding energies of tautomer **1** only, and obtained values within 260 meV of our values for the 1s ionization energies of C_5, C_8, and C_2, peaks A, B, and D, respectively. For ionization of C_6, they obtained a value which is 0.67 eV lower than ours, so that it contributes to peak C, rather than D.

III.3. Oxygen, Nitrogen, and Carbon K-Edge Photoabsorption Spectra. Before considering the experimental spectra, we briefly consider the structure of the core−hole electron excitation manifold of guanine, within the approximation of planar molecular structure (C_s symmetry). The strongest spectral maxima are essentially excitations of core electrons into vacant π^* orbitals (a'' orbitals in C_s symmetry, and involving double bonds), whose number (and corresponding valence states) can be estimated as follows. In guanine 11 atomic p_z orbitals of C, N, and O give rise to 11 a'' MOs, seven of which are occupied and four are vacant in all tautomers, **1**−**8**. The occupied a'' MOs comprise four π-type MOs due to the double bonds and three (nonbonding) MOs due to the lone pair MOs of amino nitrogen and hydroxy oxygen atoms. The four vacant MOs are the π^*-type antibonding counterparts of the occupied π-orbitals, and are labeled V_1 to V_4. Transitions to these MOs make possible four valence-type A″ excited states for each core hole, whose intensity can be roughly estimated from the spatial overlap of the MO and the core orbital.

The rest of the excitations can be considered as various members of Rydberg series with varying admixture of antibonding character. States of A′ symmetry are *n*s and *n*p Rydberg states connected to specific core holes and converging to their respective ionization thresholds. The *n*d and higher angular momentum series are not considered here due to the lack of appropriate diffuse basis functions in our calculations. Accordingly, only *n*p-type Rydberg states can be expected among a'' excited states. At this point it has to be recalled that the division of excitations into Rydberg and valence is theoretically not rigorous, and the assignments proposed in the present work are only of approximate nature. Moreover, the analysis of A″ states is complicated by possible interaction of Rydberg and π^*-valence electronic configurations. The cases where such interaction cannot be excluded are indicated by question marks in the following tables.

In Figure 5 the theoretical and experimental O 1s excitation spectra of guanine are compared, and assignments of the spectral features are given in Table 6. For the sake of brevity, only optically allowed transitions with intensity ≥0.04 of the strongest transition are included. In the figure, all calculations are included in the calculated curves, and the full list is available as Supporting Information. The same is true for the N and C K-edge spectra.

The experimental O 1s excitation spectrum of guanine is relatively simple and is dominated by the two maxima A and B at 531.7 and 535.3 eV. Our calculations indicate that A is due to transitions O 1s → V_1 of the oxo tautomers **1** and **2**. Peak B is more complex and is composed mostly of transitions from O 1s of the hydroxy forms **3** and **4** to V_1 and 3s, with a minor contribution from two tautomer **2** transitions. The complexity of peak B, with the hydroxy tautomers each

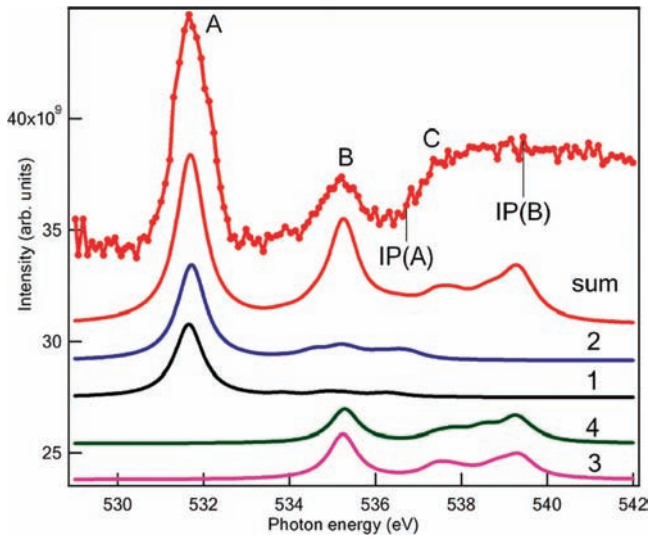

Figure 5. Experimental (points and lines) and theoretical (lines) O 1s photoabsorption spectra of guanine and its tautomers. The theoretical spectrum has been shifted by −2.22 eV, to align it with the experimental spectrum and broadened by a Lorentzian function of fwhm = 0.8 eV. Experimental ionization potentials of features A and B in Figure 2 are marked.

TABLE 6: Calculated ($I \geq 0.04$) and Experimental Energies, Oscillator Strengths f, and Relative Intensities of the Main Vertical O 1s Excitations of Guanine

Theory						Experiment	
Tautomer	Transition	Assignment	Energy Ω_t [a]	f	I	Maximum	Energy Ω_e
1	$1\,^1A''$	O 1s → V_1	531.69	0.031	0.769	A	531.7
2	$1\,^1A''$	O 1s → V_1	531.75	0.028	1.000		
2	$2\,^1A'$	O 1s → 3p	534.59	0.002	0.077	B	535.3
2	$2\,^1A''$	O 1s → V_2?	535.21	0.003	0.097		
3	$1\,^1A'$	O 1s → 3s	535.25	0.011	0.244		
3	$1\,^1A''$	O 1s → V_1	535.29	0.010	0.227		
4	$1\,^1A''$	O 1s → V_1	535.31	0.010	0.165		
4	$1\,^1A'$	O 1s → 3s	535.32	0.011	0.185		
3	$2\,^1A'$	O 1s → 3p	537.43	0.005	0.109	C	537.8
4	$2\,^1A'$	O 1s → 3p	537.46	0.004	0.064		
4	$5\,^1A'$	O 1s → 4p	538.51	0.004	0.059		
3	$5\,^1A'$	O 1s → 4p	538.75	0.002	0.052		

[a] The theoretical energies have been shifted by 2.22 eV to lower binding energy.

contributing two transitions, and overlapping a contribution from the oxo form, is consistent with the most recent assignments of the second band in formic acid. Formic acid is the simplest organic molecule that contains both an oxo and a hydroxy group, and has O 1s photoabsorption bands at 532.17 and 535.37 eV.[51] Tabayashi et al.[52] have recently carried out calculations and gave an assignment of the two bands which is quite consistent with the present results.

At higher energy the spectrum becomes more complex. Already band B contains a number of contributions from various transitions labeled 3s and 3p Rydberg (Table 6), but which probably have substantial antibonding character. Above 536 eV the spectrum is apparently dominated by Rydberg states. The higher members of the Rydberg series located here converge to ionization potentials of their respective tautomers within the energy range 536.5−539.5 eV. This part of the spectrum is therefore most likely a superposition of discrete and continuum transitions, and the latter cannot be reproduced well by the present calculations because of the basis set limitations. Our calculations tentatively assign the maximum C at about 537.80 eV to a combination of 3p and 4p Rydberg transitions in tautomers **3** and **4**. An analogous peak in formic acid at 538.37 eV was similarly assigned.[51]

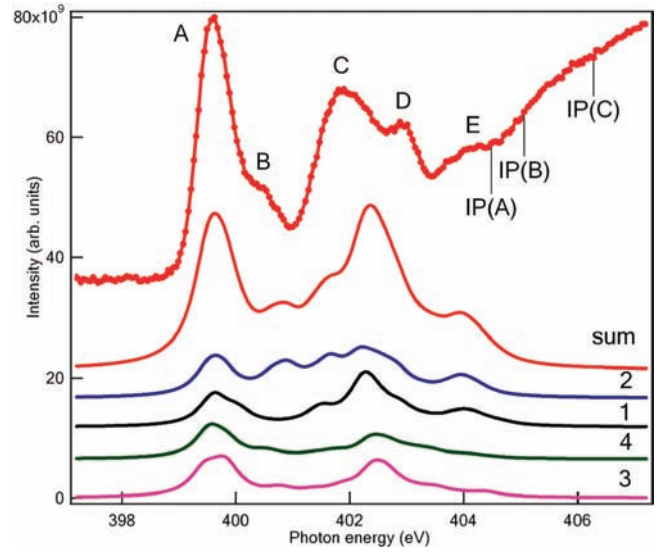

Figure 6. Experimental (points and lines) and theoretical (lines) N 1s photoabsorption spectra of guanine. The theoretical spectrum has been shifted by −2.35 eV, to align the first peak of the experimental and theoretical spectra and broadened by a Lorentzian function of fwhm = 0.6 eV. Experimental ionization potentials of features A, B, and C in Figure 3 are marked.

The N 1s excitation spectrum of guanine is rather complex (Figure 6, Table 7). Band A with high-energy shoulder B and bands C−E can clearly be seen in the experimental spectrum. All of the observed spectral structures are rather diffuse, which is in agreement with the results of our calculations predicting a high density of excited states at low energy. Many of the N 1s excitations have appreciable spectral intensities, which makes the list of transitions in Table 7 rather lengthy despite the higher selection threshold ($I \geq 0.10$) applied in this case. It is therefore not surprising that the overall shape of the experimental N 1s NEXAFS envelope is less accurately reproduced by the calculations. There is however sufficient qualitative agreement between the theoretical and experimental spectra to give at least an approximate interpretation of the spectrum.

The tautomers **1** to **4** have signals in all energy regions of the N 1s excitation spectrum, but the signatures of individual tautomers are not so clear. An exception is shoulder B at 400.5 eV of the experimental spectrum which can be assigned mainly to tautomer **2** (transitions N_3 1s → V_2 and N_9 1s → 3p). Also the band E at about 404.07 eV is assigned mainly to excitation processes in tautomers **1** and **2** (transitions N_1 1s → 3p and N_{10} 1s → 3p).

Assignment of the more prominent bands A, C, and D at 399.6, 401.86, and 402.95 eV of the experimental spectrum is less clear, since many transitions simultaneously contribute to these bands. The lowest band is attributed to excitations of 1s electrons of imino-group nitrogen atoms to final state V_1 (atoms N_3 and N_7 in tautomer **1**, atoms N_3 and N_9 in tautomer **2**, N_1, N_3, and N_7 in tautomers **3** and **4**). A substantial contribution to bands C and D is provided by amino-group nitrogen 1s → V_1 transitions (atoms N_1, N_9, N_{10} in tautomer **1**, atoms N_1, N_7, N_{10} in tautomer **2**, atoms N_9, N_{10} in tautomers **3** and **4**). These V_1 excitations can be considered as amino-type counterparts to the excitations of band A due to the imino-type nitrogen atoms.

TABLE 7: Calculated ($I \geq 0.10$) and Experimental Energies, Oscillator Strengths f, and Relative Intensities of the Main Vertical N 1s Excitations of Guanine

Theory						Experiment	
Tautomer	Transition	Assignment	Ω_t[a]	f	I	Maximum	Ω_e
3	$1\,^1A''$	$N_7\ 1s \rightarrow V_1$	399.41	0.036	0.790	A	399.6
4	$1\,^1A''$	$N_7\ 1s \rightarrow V_1$	399.49	0.033	0.533		
2	$1\,^1A''$	$N_9\ 1s \rightarrow V_1$	399.50	0.023	0.843		
4	$2\,^1A''$	$N_1\ 1s \rightarrow V_1$	399.50	0.024	0.392		
1	$1\,^1A''$	$N_7\ 1s \rightarrow V_1$	399.57	0.040	1.000		
3	$2\,^1A''$	$N_1\ 1s \rightarrow V_1$	399.71	0.021	0.449		
2	$2\,^1A''$	$N_3\ 1s \rightarrow V_1$	399.73	0.019	0.698		
4	$3\,^1A''$	$N_3\ 1s \rightarrow V_1$	399.79	0.029	0.461		
3	$3\,^1A''$	$N_3\ 1s \rightarrow V_1$	399.81	0.029	0.635		
1	$2\,^1A''$	$N_3\ 1s \rightarrow V_1$	399.98	0.017	0.424		
4	$4\,^1A''$	$N_1\ 1s \rightarrow V_2$?	400.52	0.012	0.188	B	400.5
2	$3\,^1A''$	$N_3\ 1s \rightarrow V_2$	400.60	0.011	0.414		
3	$4\,^1A''$	$N_1\ 1s \rightarrow V_2$?	400.73	0.010	0.219		
2	$4\,^1A''$	$N_9\ 1s \rightarrow 3p$?	400.86	0.019	0.693		
2	$2\,^1A'$	$N_{10}\ 1s \rightarrow 3s$	401.34	0.006	0.211	C	401.9
1	$3\,^1A''$	$N_3\ 1s \rightarrow V_2$	401.43	0.013	0.318		
1	$2\,^1A'$	$N_{10}\ 1s \rightarrow 3s$	401.48	0.005	0.138		
2	$5\,^1A''$	$N_7\ 1s \rightarrow V_1$	401.61	0.024	0.851		
4	$6\,^1A''$	$N_{10}\ 1s \rightarrow V_1$	401.68	0.009	0.152		
3	$6\,^1A''$	$N_{10}\ 1s \rightarrow V_1$	401.83	0.009	0.198		
2	$6\,^1A''$	$N_1\ 1s \rightarrow V_1$	402.08	0.017	0.605	D	402.95
1	$5\,^1A'$	$N_1\ 1s \rightarrow 3s$	402.13	0.009	0.230		
1	$5\,^1A''$	$N_1\ 1s \rightarrow V_1$	402.18	0.017	0.429		
2	$7\,^1A'$	$N_1\ 1s \rightarrow 3s$	402.21	0.009	0.340		
1	$6\,^1A''$	$N_9\ 1s \rightarrow V_1$	402.23	0.026	0.648		
4	$7\,^1A''$	$N_9\ 1s \rightarrow V_1$	402.31	0.022	0.359		
3	$7\,^1A'$	$N_9\ 1s \rightarrow 3s$	402.31	0.008	0.179		
1	$7\,^1A'$	$N_9\ 1s \rightarrow 3s$	402.35	0.008	0.213		
3	$8\,^1A''$	$N_9\ 1s \rightarrow V_1$	402.37	0.023	0.502		
4	$8\,^1A'$	$N_9\ 1s \rightarrow 3s$	402.40	0.008	0.133		
1	$7\,^1A''$	$N_{10}\ 1s \rightarrow V_1$	402.41	0.009	0.221		
2	$8\,^1A''$	$N_{10}\ 1s \rightarrow V_1$	402.44	0.008	0.287		
2	$9\,^1A'$	$N_7\ 1s \rightarrow 3s$	402.53	0.008	0.274		
3	$12\,^1A'$	$N_{10}\ 1s \rightarrow 3p$	402.58	0.016	0.353		
4	$12\,^1A'$	$N_{10}\ 1s \rightarrow 3p$	402.64	0.016	0.266		
3	$11\,^1A''$	$N_7\ 1s \rightarrow V_2$?	402.67	0.005	0.116		
2	$12\,^1A'$	$N_{10}\ 1s \rightarrow 3p$	402.78	0.015	0.546		
1	$12\,^1A'$	$N_{10}\ 1s \rightarrow 3p$	402.84	0.016	0.414		
4	$17\,^1A''$	$N_{10}\ 1s \rightarrow V_2$?	403.43	0.006	0.102	E	404.1
3	$16\,^1A''$	$N_{10}\ 1s \rightarrow V_2$?	403.47	0.007	0.152		
1	$16\,^1A'$	$N_1\ 1s \rightarrow 3p$	403.82	0.006	0.151		
2	$15\,^1A''$	$N_{10}\ 1s \rightarrow 3p$?	403.91	0.008	0.288		
2	$20\,^1A'$	$N_1\ 1s \rightarrow 3p$	403.91	0.004	0.143		
1	$15\,^1A''$	$N_{10}\ 1s \rightarrow 3p$?	404.05	0.009	0.222		

[a] The theoretical energies have been shifted by 2.35 eV.

The V_1 excitations are of course only the "main ingredients" of bands A, C, and D, and many additional excitations also contribute to these bands, some of them being quite important, Table 7.

Mochizuki et al.[53] calculated the N 1s excitation energies to π^* orbitals for tautomer **1** only. The agreement is not good, as their energies need to be shifted by values from 0 to 2.0 eV to align with experiment, and we calculate one additional transition for N3. It can be noted that one has to check whether it is possible that the use of the real nonplanar structure of guanine instead of the planar approximation adopted in our calculations could improve the agreement of the theoretical spectrum with experiment.

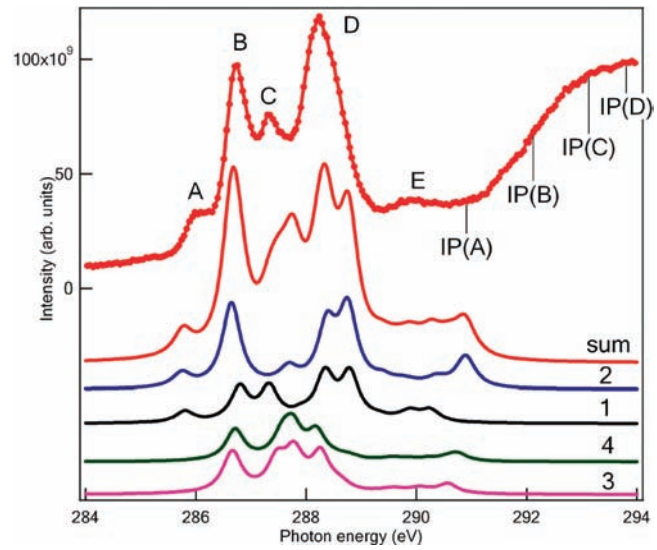

Figure 7. Experimental (points and lines) and theoretical (lines) C 1s photoabsorption spectra of guanine. The theoretical spectrum has been shifted by −2.5 eV to align it with the experimental spectrum and broadened by a Lorentzian function of fwhm = 0.4 eV. Experimental ionization potentials of features A to D in Figure 4 are marked.

The C 1s NEXAFS spectrum of guanine (Figure 7, Table 8) is dominated by two strong peaks B and D at about 286.7 and 288.2 eV, respectively, and also shows three less pronounced features A, C, and E at about 286.0, 287.3, and 289.9 eV, respectively. The calculated spectrum is in good qualitative agreement with the results of the measurements. There are some discrepancies in the region of peak D, where our calculations predict a double maximum structure.

The lowest maximum A is assigned to C_5 1s → V_1 transitions of tautomers **1** and **2**, while the next band B contains contributions of all four guanine tautomers. The main type of transition found here is 1s → V_1, where excitation takes place from atoms C_4, C_8 (tautomers **1** and **2**) and C_8 (tautomers **3** and **4**). An appreciable contribution to the intensity of band B is given by transitions C_5 1s → V_2 (tautomers **3** and **4**).

Band C of the C 1s NEXAFS spectrum is interpreted as a complex mixture of transitions C_4 1s → V_1 and C_6 1s → V_1 in tautomers **3** and **4** and various 3p Rydberg excitations. The spectra of all principle tautomers **1**−**4** contribute to this spectral region substantially. Band D also contains contributions from all types of excitations and tautomers but is mostly a result of V_1 excitations from atoms C_2 and C_6 in tautomers **1** and **2**, with contributions of C_2 1s → V_1 excitations of tautomers **3** and **4**. The low intensity maximum E near the ionization thresholds is due to tautomers **1**−**4**. No prominent transitions can be found among the various Rydberg and valence transitions contributing to this spectral region.

The C 1s X-ray absorption spectrum has been calculated by Moewes et al.[54] for tautomer **1** only and compared with measurements of spectra of condensed guanine. The chief difference with respect to our calculation is the absence of peak A in their calculation, although this peak was also present in their experimental spectra. This indicates our calculations are more reliable, since band A is characteristic of tautomer **1**. Tautomer **2** also has a structure at this energy and both **1** and **2** contribute to band D. The other spectral features are less individual and represent mixtures of excitation spectra of the tautomers **1** to **4**.

TABLE 8: Calculated ($I \geq 0.05$) and Experimental Energies, Oscillator Strengths f, and Relative Intensities of the Main Vertical C 1s Excitations of Guanine

Theory						Experiment	
Tautomer	Transition	Assignment	Ω_t[a]	f	I	Maximum	Ω_e
2	$1\,^1A''$	$C_5\ 1s \rightarrow V_1$	285.85	0.014	0.217	A	286.0
1	$1\,^1A''$	$C_5\ 1s \rightarrow V_1$	285.90	0.016	0.169		
3	$2\,^1A''$	$C_5\ 1s \rightarrow V_2$?	286.71	0.023	0.209	B	286.7
2	$2\,^1A''$	$C_4\ 1s \rightarrow V_1$	286.73	0.030	0.454		
2	$3\,^1A''$	$C_8\ 1s \rightarrow V_1$	286.75	0.057	0.862		
3	$3\,^1A''$	$C_8\ 1s \rightarrow V_1$	286.78	0.049	0.441		
4	$2\,^1A''$	$C_5\ 1s \rightarrow V_2$?	286.79	0.019	0.129		
4	$3\,^1A''$	$C_8\ 1s \rightarrow V_1$	286.82	0.052	0.350		
1	$2\,^1A''$	$C_8\ 1s \rightarrow V_1$	286.89	0.045	0.472		
1	$4\,^1A''$	$C_4\ 1s \rightarrow V_1$	287.43	0.049	0.513		
3	$4\,^1A''$	$C_4\ 1s \rightarrow V_1$	287.57	0.050	0.456	C	287.3
4	$4\,^1A''$	$C_4\ 1s \rightarrow V_1$	287.67	0.049	0.329		
2	$4\,^1A''$	$C_5\ 1s \rightarrow 3p$?	287.79	0.016	0.243		
4	$5\,^1A''$	$C_5\ 1s \rightarrow 3p$?	287.83	0.009	0.062		
4	$6\,^1A''$	$C_6\ 1s \rightarrow V_1$	287.86	0.061	0.415		
3	$5\,^1A''$	$C_6\ 1s \rightarrow V_1$	287.87	0.059	0.534		
1	$5\,^1A''$	$C_5\ 1s \rightarrow V_2$?	288.01	0.008	0.082		
3	$6\,^1A''$	$C_5\ 1s \rightarrow 3p$?	288.01	0.008	0.075		
4	$7\,^1A''$	$C_2\ 1s \rightarrow V_1$	288.29	0.061	0.415	D	288.2
3	$7\,^1A''$	$C_2\ 1s \rightarrow V_1$	288.36	0.062	0.563		
5	$6\,^1A''$	$C_2\ 1s \rightarrow V_1$	288.37	0.060	0.057		
1	$7\,^1A''$	$C_6\ 1s \rightarrow V_1$	288.44	0.061	0.638		
2	$5\,^1A''$	$C_6\ 1s \rightarrow V_1$	288.47	0.059	0.885		
1	$5\,^1A'$	$C_8\ 1s \rightarrow 3s$	288.53	0.007	0.069		
2	$7\,^1A''$	$C_4\ 1s \rightarrow V_2$?	288.74	0.005	0.071		
3	$5\,^1A'$	$C_8\ 1s \rightarrow 3s$	288.75	0.007	0.066		
2	$9\,^1A''$	$C_2\ 1s \rightarrow V_1$	288.85	0.066	1.000		
4	$4\,^1A'$	$C_8\ 1s \rightarrow 3s$	288.89	0.008	0.052		
1	$9\,^1A''$	$C_2\ 1s \rightarrow V_1$	288.89	0.068	0.713		
2	$5\,^1A'$	$C_8\ 1s \rightarrow 3s$	288.91	0.007	0.102		
2	$10\,^1A''$	$C_4\ 1s \rightarrow 3p$?	289.50	0.005	0.075	E	289.90
1	$12\,^1A''$	$C_5\ 1s \rightarrow V_4$?	289.96	0.006	0.064		
1	$13\,^1A''$	$C_8\ 1s \rightarrow 3p$?	289.97	0.006	0.063		
2	$15\,^1A''$	$C_8\ 1s \rightarrow V_2$?	290.47	0.006	0.095		
3	$19\,^1A''$	$C_5\ 1s \rightarrow V_4$?	290.68	0.013	0.121		
4	$19\,^1A''$	$C_5\ 1s \rightarrow V_4$?	290.87	0.011	0.078		

[a] The theoretical curves have been shifted by −2.50 eV.

Lastly we present wide scan photoabsorption spectra at all three edges, nitrogen, carbon, and oxygen, in Figure 8. At all edges, there are broad maxima at 7−10 eV above the first resonance and structures that extend to higher energies. These are generally attributed to various σ resonances.

IV. Conclusions

The relative energies of the tautomers of guanine have been calculated to high accuracy to yield quantitative predictions of the Boltzmann population ratios. The core level photoemission spectra have been measured at 600 K, at thermal equilibrium, and have also been theoretically calculated. The results are in good quantitative agreement for the intensities, thus confirming the calculated Boltzmann population ratios. The energies are in good overall agreement, with the theoretical energy scale for C 1s being expanded with respect to experiment. The C, N, and O K-edge photoabsorption spectra have been measured and calculated, and there is good qualitative agreement for the C and O edges, with only moderate agreement for the N K-edge. Overall the accuracy of our calculated Boltzmann population ratios is strongly supported by our measurements.

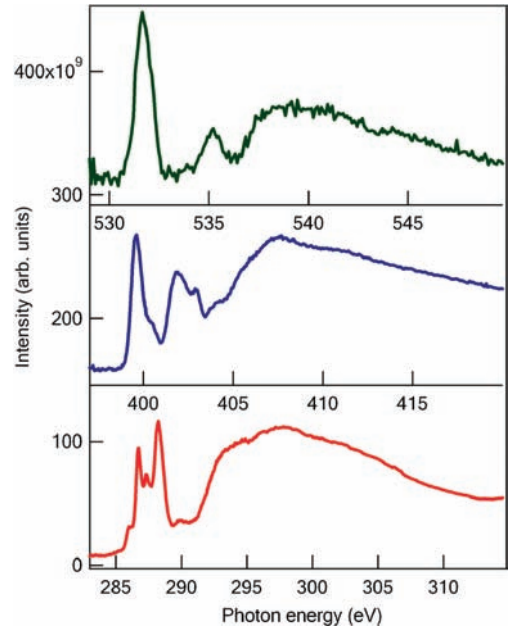

Figure 8. Wide scan NEXAFS spectra at the C, N, and O K-edge of guanine.

Acknowledgment. The theoretical part of this study was supported by grants from the Russian Foundation for Basic Research (RFBR) and the Deutsche Forschungsgemeinschaft (DFG). We gratefully acknowledge the assistance of our colleagues at Elettra for providing good quality synchrotron light. O. Plekan acknowledges financial support from the Area di Ricerca di Trieste under the Incoming Mobility scheme. V. Feyer thanks the Abdus Salaam International Center for Theoretical Physics for a TRIL (Training and Research in Italian Laboratories) fellowship. A. B. Trofimov gratefully acknowledges support from the Alexander von Humboldt Foundation.

Supporting Information Available: Complete ref 48, ground state geometries of guanine tautomers (Figure 1) optimized at the MP2/cc-pVTZ level of theory, a complete list of calculated energies, pole strengths, and photoelectron intensities of the vertical O 1s, N 1s, and C 1s ionization transitions of guanine tautomers, and a complete list of calculated energies, oscillator strengths, and relative intensities of the vertical O 1s, N 1s, and C 1s excitations of guanine tautomers. This material is available free of charge via the Internet at http://pubs.acs.org.

References and Notes

(1) Choi, M. Y.; Miller, R. E. *J. Am. Chem. Soc.* **2006**, *128*, 7320.
(2) Choi, M. Y.; Miller, R. E. *J. Phys. Chem. A* **2007**, *111*, 2475.
(3) Piuzzi, F.; Mons, M.; Dimicoli, I.; Tardivel, B.; Zhao, Q. *Chem. Phys.* **2001**, *270*, 205.
(4) Nir, E.; Plützer, Ch.; Kleinermanns, K.; de Vries, M. *Eur. Phys. J. D* **2002**, *20*, 317.
(5) Plekan, O.; Feyer, V.; Richter, R.; Coreno, M.; de Simone, M.; Prince, K. C.; Trofimov, A. B.; Gromov, E. V.; Zaytseva, I. L.; Schirmer, *J. Chem. Phys.* **2008**, *347*, 360.
(6) Mons, M.; Dimicoli, I.; Piuzzi, F.; Tardivel, B.; Elhanine, M. *J. Phys. Chem. A* **2002**, *106*, 5088.
(7) Szczesniak, M.; Szczesniak, K.; Kwiatkowski, J. S.; KuBulat, K.; Person, W. B. *J. Am. Chem. Soc.* **1988**, *110*, 8319.

(8) Hanus, M.; Ryjáček, F.; Kabeláč, M.; Kubar, T.; Bogdan, T. V.; Trygubenko, S. A.; Hobza, P. *J. Am. Chem. Soc.* **2003**, *125*, 7678.

(9) Marian, C. M. *J. Phys. Chem. A* **2007**, *111*, 1545.

(10) Nir, E.; Janzen, Ch.; Imhof, P.; Kleinermans, K.; de Vries, M. S. *J. Chem. Phys.* **2001**, *115*, 4604.

(11) Pugliesi, I.; Müller-Dethlefs, K. *J. Phys. Chem. A* **2006**, *110*, 13045.

(12) Chen, H.; Li, S. *J. Phys. Chem. A* **2006**, *110*, 12360.

(13) Shukla, M. K.; Leszczynski, J. *Chem. Phys. Lett.* **2006**, *429*, 261.

(14) Zhou, J.; Kostko, O.; Nicolas, C.; Tang, X.; Belau, L.; de Vries, M. S.; Ahmed, M. *J. Phys. Chem. A* **2009**, *113*, 4829.

(15) Feyereisen, M.; Fitzgerald, G.; Komornicki, A. *Chem. Phys. Lett.* **1993**, *208*, 359.

(16) Dunning, T. H. J. *Chem. Phys.* **1989**, *90*, 1007. Kendall, R. A.; Dunning, T. H.; Harrison, R. J. *J. Chem. Phys.* **1992**, *96*, 6796.

(17) Becke, A. D. *J. Chem. Phys.* **1993**, *98*, 5648. Lee, C.; Yang, W.; Parr, R. G. *Phys. Rev. B* **1988**, *37*, 758.

(18) Schäfer, A.; Huber, C.; Ahlrichs, R. *J. Chem. Phys.* **1994**, *100*, 5829.

(19) Grimme, S.; Waletzke, M. *J. Chem. Phys.* **1999**, *111*, 5645.

(20) Brown, R. S.; Tse, A.; Vederas, J. C. *J. Am. Chem. Soc.* **1980**, *102*, 1174.

(21) Francis, J. T.; A. P; Hitchcock, J. T. *J. Phys. Chem.* **1994**, *98*, 3650.

(22) Haranczyk, M.; Gutowski, M. *J. Am. Chem. Soc.* **2005**, *127*, 699.

(23) Trofimov, A. B.; Schirmer, J.; Kobychev, V. B.; Potts, A. W.; Holland, D. M. P.; Karlsson, L. *J. Phys. B: At., Mol. Opt. Phys.* **2006**, *39*, 305.

(24) Lin, J.; Yu, C.; Peng, S.; Akiyama, I.; Li, K.; Lee, L. K.; LeBreton, P. R. *J. Phys. Chem.* **1980**, *84*, 1006.

(25) Nir, E.; Janzen, Ch.; Imhof, P.; Kleinermanns, K.; de Vries, M. S. *J. Chem. Phys.* **2001**, *115*, 4604.

(26) Dougherty, D.; Younathan, E. S.; Voll, R.; Abdulnur, S.; McGlynn, S. P. *J. Electron Spectrosc. Relat. Phenom.* **1978**, *13*, 379.

(27) Feyer, V.; Plekan, O.; Richter, R.; Coreno, M.; Vall-llosera, G.; Prince, K. C.; Trofimov, A. B.; Zaytseva, I. L.; Moskovskaya, T. E.; Gromov, E. V.; Schirmer, J *J. Phys. Chem. A* **2009**, *113*, 5736.

(28) Prince, K. C.; Blyth, R. R.; Delaunay, R.; Zitnik, M.; Krempasky, J.; Slezak, J.; Camilloni, R.; Avaldi, L.; Coreno, M.; Stefani, G.; Furlani, C.; de Simone, M.; Stranges, S. *J. Synchrotron Radiat.* **1998**, *5*, 565.

(29) Thomas, T. D.; Shaw, R. W., Jr. *J. Electron Spectrosc. Relat. Phenom.* **1974**, *5*, 1081.

(30) Myrseth, V.; Bozek, J. D.; Kukk, E.; Sæthre, L. J.; Thomas, T. D. *J. Electron Spectrosc. Relat. Phenom.* **2002**, *122*, 57.

(31) Plekan, O.; Feyer, V.; Richter, R.; Coreno, M.; de Simone, M.; Prince, K. C.; Carravetta, V. *J. Electron Spectrosc. Relat. Phenom.* **2007**, *155*, 47–53.

(32) Schirmer, J.; Cederbaum, L. S.; Walter, O. *Phys. Rev. A* **1983**, *28*, 1237.

(33) von Niessen, W.; Schirmer, J.; Cederbaum, L. S. *Comp. Phys. Rep.* **1984**, *1*, 57.

(34) Schirmer, J.; Angonoa, G. *J. Chem. Phys.* **1989**, *91*, 1754.

(35) Cederbaum, L. S.; Domcke, W.; Schirmer, J. *Phys. Rev. A* **1980**, *22*, 206.

(36) Angonoa, G.; Walter, O.; Schirmer, J. *J. Chem. Phys.* **1987**, *87*, 6789.

(37) Hehre, W. J.; Ditchfield, R.; Pople, J. A. *J. Chem. Phys.* **1972**, *56*, 2257.

(38) Clark, T.; Chandrasekhar, J.; v. R. Schleyer, P. *J. Comput. Chem.* **1983**, *4*, 294.

(39) One-particle Green's function ADC(4)/CVS code written by G. Angonoa, O. Walter, J. Schirmer; direct treatment of the first-order matrix elements and diagonalization due to F. Tarantelli. The constant diagram code written by G. Angonoa, O. Walter and J. Schirmer; further developed by M. K. Scheller and A. B. Trofimov.

(40) Program written by Guest, M. F.; van Lenthe, J. H.; Kendrick, J.; Schoffel, K.; Sherwood, P. with contributions fromAmos, R. D.; Buenker, R. J.; Dupuis, M.; Handy, N. C.; Hiller, I. H.; Knowles, P. J.; Bonacic-Koutecky, V.; von Niessen, W.; Harrison, R. J.; Rendell, A. P.; Saunders, V. R.; Stone, A. J. The package is derived from the original GAMESS code due toDupuis, M.; Spangler, D.; Wendoloski, J. NRCC Software Catalog, Vol. 1, Program No. QG01 (GAMESS), 1980.

(41) Schmidt, M. W.; Baldridge, K. K.; Boatz, J. A.; Elbert, S. T.; Gordon, M. S.; Jensen, J. H.; Koseki, S.; Matsunaga, N.; Nguyen, K. A.; Su, S. J.; Windus, T. L.; Dupuis, M.; Montgomery, J. A. *J. Comput. Chem.* **1993**, *14*, 1347.

(42) Schirmer, J. *Phys. Rev. A* **1982**, *26*, 2395.

(43) Trofimov, A. B.; Schirmer, J. *J. Phys. B: At. Mol. Phys.* **1995**, *28*, 2299.

(44) Barth, A.; Schirmer, J. *J. Phys. B: At. Mol. Phys.* **1985**, *18*, 867.

(45) Polarization propagator ADC code written by Trofimov, A. B. Stelter, G. Schirmer, J.

(46) Becke, A. D. *J. Chem. Phys.* **1993**, *98*, 5648. Lee, C.; Yang, W.; Parr, R. G *Phys. Rev. B* **1988**, *37*, 758.

(47) Krishnan, R.; Binkley, J. S.; Seeger, R.; Pople, J. A. *Chem. Phys.* **1980**, *72*, 650.

(48) Frisch, M. J.; et al. *Gaussian 98, Revision A.7*; Gaussian, Inc.: Pittsburgh, PA, 1998.

(49) Jolly, W. L.; Bomben, K. D.; Eyermann, C. J. *At. Data Nucl. Data Tables* **1984**, *31*, 433.

(50) Takahata, Y.; Okamoto, A. K.; Chong, D. P. *Int. J. Quantum Chem.* **2006**, *106*, 2581.

(51) Prince, K. C.; Richter, R.; de Simone, M.; Coreno, M. *J. Phys. Chem. A* **2003**, *107*, 1955.

(52) Tabayashi, K.; Yamamoto, K.; Takahashi, O.; Tamenori, Y.; Harries, J. R.; Gejo, T.; Iseda, M.; Tamura, T.; Honma, K. *J. Chem. Phys.* **2006**, *125*, 194307.

(53) Mochizuki, Y.; Koide, H.; Imamura, T.; Takemiya, H. *J. Synchrotron Radiat.* **2001**, *8*, 1003.

(54) Moewes, A.; MacNaughton, J.; Wilks, R.; Lee, J. S.; Wettig, S. D.; Kraatz, H.-B.; Kurmaev, E. Z. *J. Electron Spectrosc. Relat. Phenom.* **2004**, *137−140*, 817.

JP903209T